Scanning Electron Microscopy

Volume 1986
Number 1 *Part I*

Article 5

4-21-1986

Computer Simulation and Experimental Performance Data for an Electron Spectrometer for Electron Beam Testing of Integrated Circuits

D. Deutges
Universität Duisburg

S. Görlich
Universität Duisburg

E. Kubalek
Universität Duisburg

SCANNING ELECTRON MICROSCOPY/1986/I (Pages 45-56)
SEM Inc., AMF O'Hare (Chicago), IL 60666-0507 USA

0586-5581/86$1.00+05

COMPUTER SIMULATION AND EXPERIMENTAL PERFORMANCE DATA FOR AN ELECTRON SPECTROMETER FOR ELECTRON BEAM TESTING OF INTEGRATED CIRCUITS

D. Deutges, S. Görlich[+] and E. Kubalek

Universität Duisburg, Fachgebiet Werkstoffe der Elektrotechnik
Leiter: Prof. Dr.-Ing. Erich Kubalek
Kommandantenstr. 60
D 4100 Duisburg 1, F.R.G.

[+]Present address: Siemens AG ZT ZFE, Otto Hahn Ring 6, ME23
D-8000 Munchen 83, FRG

(Received for publication February 05, 1986, and in revised form April 21, 1986)

Abstract

Electron beam testing using voltage contrast in the scanning electron microscope has been established as a useful tool for nondestructive and nonloading functional testing and failure analysis of integrated circuits (IC). The accuracy of quantitative voltage measurements within the IC with the electron beam probe is determined by the performance of the secondary electron (SE) spectrometer used.

For simulating the performance of SE-spectrometers a program-package has been developed by aid of which the voltage- and field-distributions within the spectrometers can be evaluated using a finite element method. Thus it is possible to trace electron trajectories throughout the spectrometer. By considering a great number of SE-trajectories, the detected integral SE-signal for different voltages at the IC can be determined as a function of the retarding field voltage within the spectrometer. In this way the performance of an existing spectrometer is simulated.

The experimentally measured SE-signals are compared with the simulation data. This comparison showed that the program-package realistically simulates the spectrometer properties. Therefore this program-package enables an improvement of existing SE-spectrometers and in principle also the development of new spectrometer-assemblies. Here the suitability for optimizing a SE-spectrometer is shown.

KEY WORDS: Scanning electron microscopy, secondary electrons, voltage contrast, electron beam test techniques, integrated circuits, spectrometer, field calculations, electron trajectories, secondary electron transmission, computer aided optimization.

Address for correspondence:

E. Kubalek, Universität Duisburg, Fachgebiet Werkstoffe der Elektrotechnik,Kommandantenstr.60 4100 Duisburg 1,F.R.G. (Phone No. (0203) 379-3406

Introduction

At present various electron beam test techniques for large scale and very large scale IC exist which allow IC-internal function control as well as IC-internal failure analysis (e.g. logic state analysis or quantitative signal measurements). Surveys of electron beam testing techniques for IC are given by Menzel and Kubalek (1981), Kubalek and Menzel (1984) and Feuerbaum (1983).

In principle, these techniques are based on the fact that SE emitted from the specimen surface gain different kinetic energies between the specimen and the SE-detector, if the specimen voltage is varied. Due to micro-field potential barriers on the surface of the operating IC, the variation of the specimen voltage results in a modulation of the measured SE-signal (qualitative voltage contrast). If a SE-spectrometer with a calibrated potential barrier is used, a well defined correlation between measured SE-signal and specimen voltage exists and quantitative measurements of specimen voltages are possible. Especially for these quantitative voltage measurements, the undesired influence of microfields (i.e., fields caused by voltage differences between the measurement point and its surroundings) on the SE-trajectories (local field effects) has to be reduced as far as possible by an extraction field which has to be provided by the used SE-spectrometer.

As for IC-internal signal measurements it is intended to obtain simultaneously optimum values of spatial, time and voltage resolution, the SE-spectrometer has to be optimized with respect to the reduction of local field effects, to the improvement of the signal to noise ratio, and to minimizing the influence on the primary electron beam.

In recent years, apart from many experimental attempts, Feuerbaum (1979), Wolfgang et. al. (1979), Ura et al. (1982), Ostrow et al. (1982), Menzel and Kubalek (1983 a,b) also theoretical efforts, Goto et al. (1981), Fujioka et al. (1981), Adachi et al. (1981), Khursheed and Dinnis (1983, 1984), Deutges and Kubalek (1983) have been made to find SE-spectrometers which are optimally suited for special testing functions.

The theoretical simulation methods used un-

til now are based on simple analytical models and exclude therefore a complete quantitative description of the spectrometer properties (Goto et al. 1981; Fujioka et al. 1981). Kursheed and Dinnis (1983, 1984), on the other hand, applied the more powerful method of finite differences for the determination of the voltage distribution within the spectrometer. Thus a complete quantitative description of the spectrometer properties is possible. This method, however, does not incorporate materials with different permittivities, which should be a drawback especially for the development of new spectrometer designs. Dinnis and Kursheed (1985) and Deutges and Kubalek (1983) have used the method of finite elements which allows this incorporation and so overcomes this drawback. Based on the earlier results of Deutges and Kubalek (1983), here the simulation technique is extended, enabling now the complete evaluation of the spectrometer properties. For proving the capability of this simulation technique, a design based on an existing SE-spectrometer is used. The detected SE-signal for different specimen voltages is simulated and compared with experimental data. As a consequence of these simulation data new ideas for further improvements of SE-spectrometers for electron beam testing of IC are deduced, which led to the simulation of an improved SE-spectrometer-design changed according to these ideas.

The comparison of the simulation data with experimental data as well as the comparison of the simulation data for the two variants confirm that the presented computation technique can be used as a powerful tool for the optimization of electron spectrometers.

Experimental

In the following a SE-spectrometer assembly is presented. Its quality for quantitative signal measurements is determined experimentally. The design of this assembly is the basis for the simulations performed afterwards. In figure 1 the cross-section and some views of the experimental set up are shown.

In order to reduce the local field effects, the SE, which are generated by the primary electron beam impinging on the IC-surface, first are accelerated by an extraction field. Then they are decelerated again by the retarding grid before entering the deflection field provided by a cylindrical 127°-capacitor. Due to the voltage applied to the capacitor plates, only SE of energy within a limited range can pass the capacitor to the exit grid and thus reach the conventional Everhart-Thornley-detector. By this construction a quite homogeneous extraction-field and a small deflection-field strength are achieved so that a deformation of the primary electron beam and thus a decrease in spatial resolution practically is avoided.

The characterizing and most important property of a spectrometer is its voltage resolution. This can be determined experimentally after Gopinath (1977). The minimum detectable voltage difference ΔV depends on the least ac-

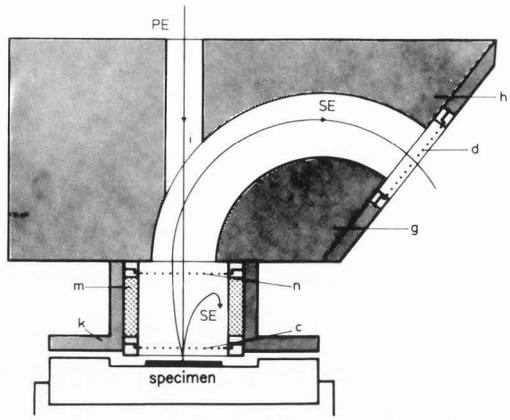

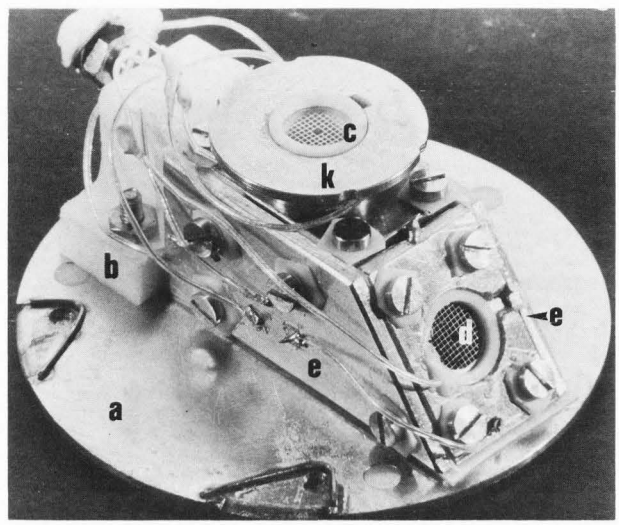

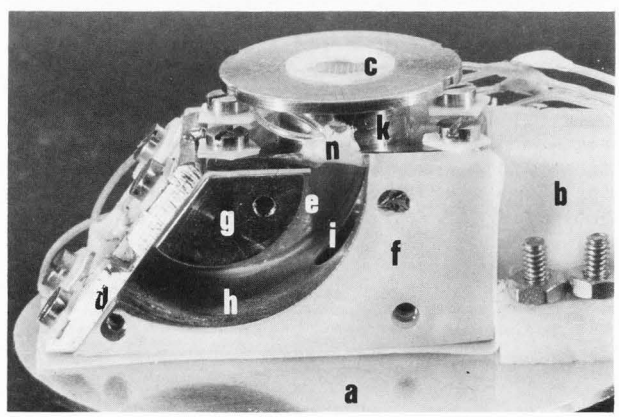

Fig. 1: Cross-section and some views of the spectrometer with:
<a> base plate, <b> teflon-mount, <c> extraction grid with ceramic holder, <d> capacitor exit grid with ceramic holder and exit plate of the cylindrical 127° deflection capacitor, <e> shielding plates for the capacitor, <f> teflon-insulation, <g> inner plate of deflection capacitor, <h> outer plate of deflection capacitor, <i> hole for primary electron beam, <k> cylindrical casing, <m> ring made of ceramic or stainless steel, <n> retarding grid with ceramic holder.

ceptable signal to noise ratio n, the detection bandwidth f and the used primary electron current I_{PE}:

$$\Delta V = Cn\sqrt{f/I_{PE}} \qquad (1)$$

The factor C in this formula determines the quality of the spectrometer: A smaller C results in a better voltage resolution. For estimating this spectrometer constant, a small square-wave voltage with ΔV = 100 mV was applied to the specimen and the detected SE-signal was measured (see fig. 2). Its peak to peak signal to noise ratio is about 3, the signal frequency is 0.1 MHz, the primary electron current, measured with a Faraday cage, is 50 nA. Inserting these values into the Gopinath formula (1), the constant is calculated to be $C=2.4\times10^{-8}\ V\sqrt{As}$, which is certainly an upper limit for the spectrometer constant, because the peak to peak value of the signal to noise ratio is lower than the normally used rms value and because the signal frequency is lower than the detection band-width. This value for C is by a factor of about 10 lower than reported by Menzel and Brunner (1983) for a Feuerbaum type spectrometer ($C=2.2\times10^{-7}\ V\sqrt{As}$), but it is still a factor 2 superior in comparison with a former 127°-spectrometer of Menzel and Kubalek (1983b) ($C=4\times10^{-8}\ V\sqrt{As}$).

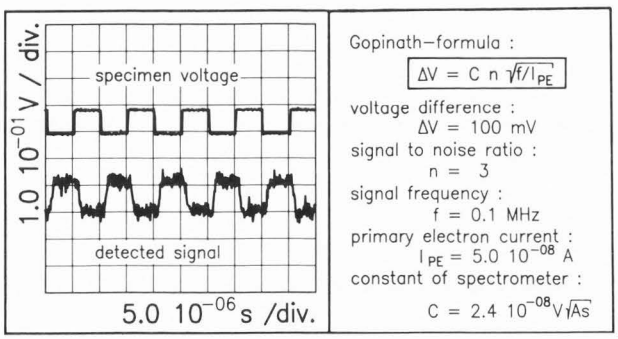

Fig. 2: Determination of the spectrometer-constant C

Computer simulation

The simulation process, Deutges and Kubalek (1983), includes the following steps:

Evaluation of the potential distribution within the spectrometer

With regard to obtaining the SE-signal curves, this has to be done for several different values of the retarding-grid voltage. For each value of the retarding-grid voltage a boundary value problem of Laplace's differential equation $\Delta V = 0$ has to be solved. This can be achieved by minimizing the electrostatic energy

$$W_{el} = \frac{1}{2}\iiint_{\text{spectrometer}} \vec{E}(\vec{r})\cdot\vec{D}(\vec{r})\ d^3r = \frac{1}{2}\iiint_{\text{spectrometer}} \epsilon(\vec{r})\cdot(\vec{\nabla}V)^2 d^3r \qquad (2)$$

which is stored within the spectrometer. For this minimizing purpose a finite element method is used, Munro (1973). Compared with the finite difference method used by Khursheed and Dinnis (1983) or the charge density method, Steinbigler (1969), Singer (1973), this method has the advantage that different permittivities within the spectrometer (insulations, mounts etc.) can be considered. As a fully 3-dimensional evaluation of the potential distribution would exceed the capability of the computer used (Hewlett Packard 1000), only such designs are chosen which can be constructed from parts with axial or translational symmetry. To calculate the potential distribution in one of these parts, its cross-sectional area is covered with a rectangular net of 101 x 81 = 8181 meshes. These rectangles are now divided into triangular "finite elements" within which the potential is assumed to vary linearly (finite element approximation). If the values of the potential distribution are known on the boundaries of the spectrometer, the minimizing of the energy-functional (eq. 2) then leads to a set of linear algebraical equations inter-relating each of the unknown mesh-point potentials with the potentials at the adjacent four mesh-points. The mesh-point potentials can be arranged easily in such an order that the coefficient matrix for the set of equations has a sparse banded structure and that the system may be solved by successive Gaussian elimination of submatrices. The accuracy of the so evaluated mesh-point potentials can be estimated. Therefore, on the boundaries of the spectrometer-design values of an analytically known potential distribution (e.g. of point charges on the axis) are taken instead of the actually applied voltages. The other mesh-point potentials are calculated using the finite element method as described above. This quality test was done for the design presented here. The maximum relative error was less than 0.01%

Calculation of electron trajectories

For the simulation of the spectrometer performance a large number of electron trajectories has to be traced within the evaluated potential distribution. Therefore the computer programs are organized so that many electron trajectories with different predefined initial conditions can be calculated. The accuracy is determined by the length of the path between two points of an electron trajectory ("stepwidth"), on which a uniformly accelerated motion due to the field strength at the previous point on the trajectory is assumed. This stepwidth is adapted optimally to the linear variation of the voltage within the triangular finite elements used for the evaluation of the voltage-distribution. The programs were tested by means of a central force problem using cylindrical coordinates. In accordance with the finite element discretisation, the analytical potential distribution of a positive point charge Q_+ was given only on the mesh nodes of the rotational cross-section shown in figure 3a. The circular and elliptical electron orbits calculated with the programs are graphed in fig. 3b. Thereby also the effects of different initial conditions (electron velocity, off

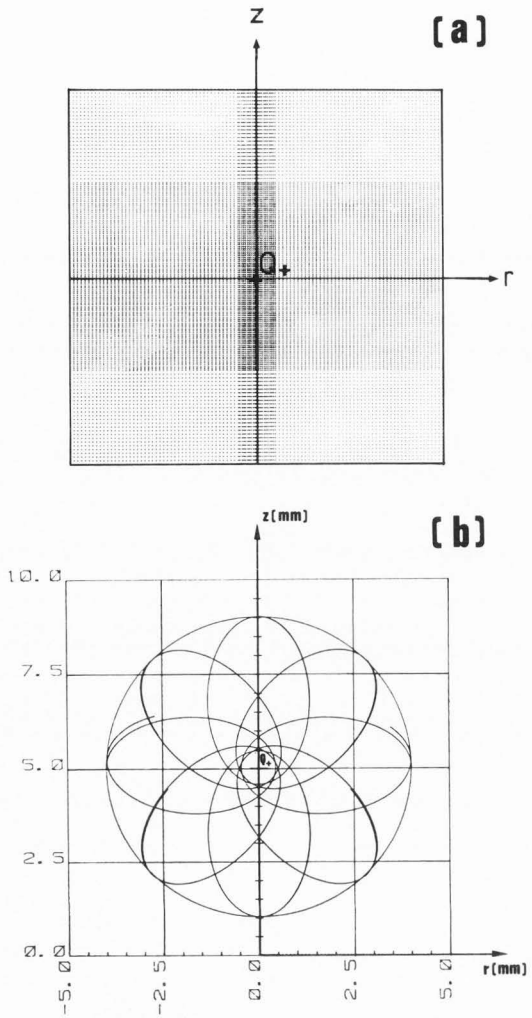

Fig. 3: Test of programs for the calculations of electron trajectories by means of a central force problem. Further explanations are given within the main text.

axis angle θ_o, azimuthal angle φ_o) on the accuracy could be examined. The small inaccuracies for some of the narrower ellipses in figure 3b can be explained by the discretisation of the voltage especially near the point charge, where the mesh width of the used finite element net is too large in respect to the high field gradient there.

Simulation of the transmission characteristic

The simulation of the transmission characteristic of the spectrometer for different retarding grid voltages is based on three assumptions:

- The SE emitted from a conductor track of an IC as a reponse to the incident primary electron beam have a kinetic energy spectrum which is independent of the voltage applied to the IC-surface.
- The primary electron beam impinges perpendicularly to the surface of the conductor track.
- If the Z-axis is defined to have a direction opposite to that of the impinging primary electron beam and if spherical coordinates are considered, then it is reasonable to assume a uniform SE-distribution for the azimuth angles φ_o and a Lambert-cosine distribution for the polar angles θ_o to the Z-axis.

On the basis of these assumptions, the following procedure was chosen in order to achieve a realistic simulation for the SE-transmission as a function of the SE-energy: For each considered SE-energy 100 SE were traced, starting from the conductor track with the azimuth angle φ_o varying from 0° to 180° in steps of 45° and the angle θ_o varying from θ_o^{1}=0° to θ_o^{20}=90° in such steps, that:

$$\int_{\theta_o^i}^{\theta_o^{i+1}} \cos\theta \, d\theta = 0.05 \qquad (i=1...19) \qquad (3)$$

Considering the symmetric properties of the design, this choice of SE gives a sufficient modelling of the angular distribution of all SE having the considered initial kinetic energy. If one of these 100 SE reached the detector, a contribution of 1% to the transmission ratio was associated, thereby taking into account the uniform distribution of the azimuth angles φ_o and the Lambert-cosine distribution of the angles θ_o in such a way that the calculated transmission ratio is scaled to 100%, if all 100 SE reach the detector. A transmission-curve $T_{SE}(E)$ now can be obtained by calculating the transmission ratio for 10 different SE-energies for each set of voltages applied to the IC and the spectrometer.

Simulation of the total detected SE-signal

The transmission characteristic is used to simulate the total detected SE-signal as a function of the retarding grid voltage. To this end, for different retarding grid voltages U_R, the transmission curves $T_{SE}(E, U_R)$ have to be convoluted with the SE-energy-spectrum $I_{SE}(E)$. After Chung and Everhart (1974) a spectrum

$$I_{SE}(U_R) \sim (E-E_F-\Phi)/(E-E_F)^4 \qquad (4)$$

with the Fermi-level E_F and the work-function Φ was chosen, and in the simulations, experimental values $E_F+1.\bar{3}\Phi$ =1.$\bar{3}$ eV and Φ= 4 eV for an aluminium surface were used. Now the total SE-transmission of the spectrometer for the applied retarding grid voltage U_R is given by:

$$T_{tot}(U_R) = \frac{\int_0^\infty I_{SE}(E)T_{SE}(E,U_R)dE}{\int_0^\infty I_{SE}(E)dE} \cdot 100\% \qquad (5)$$

Note, that $T_{tot}(U_R)$ is directly proportional to the expected detectable SE-signal and that therefore the whole simulation technique can be tested experimentally.

Model

In figure 4 the model of the spectrometer and detector assembly is shown in a cross-section for which the simulations were performed. Regarding the comparison with experimental data, it is chosen to be as similar as possible to the experimental set up of figure 1.

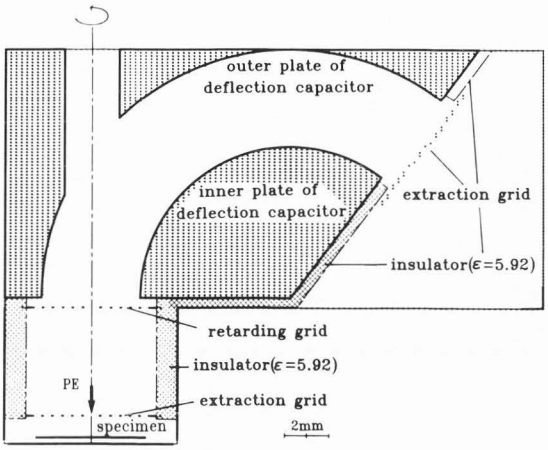

Fig.: 4 Cross-section of the simulated spectrometer.

As the simulation technique is 2-dimensional, the spectrometer was modelled by two parts: A rotationally symmetrical part with specimen, extraction grid, retarding grid, ceramic insulator, and a translationally symmetrical part with the cylindrical 127°-deflection capacitor and another extraction grid. The dots in figure 4 mark those nodes of the finite elements mesh on which the values of the voltage are known and consequently provide the boundary conditions for the calculation. The influence of the Everhart-Thornley detector is simulated by some positive voltage on the right hand bottom of the translationally symmetrical part of the model-design.

Results of the simulation

Equipotential lines and electric field pattern

In figures 5a,b the equipotential lines and electric field patterns are given for the model design for two special sets of voltages applied to the different parts of the spectrometer. Figures 5a and 5b differ only in the voltage applied to the casing of the rotationally symmetrical part. Comparing the field patterns, it can be seen that, by applying a negative voltage to the casing, the radial component of the field strength increases, and that, therefore, an enlarged electrostatic focusing action on the SE is to be expected.

Electron trajectories

In figure 6b some simulated SE-paths within the spectrometer are graphed for the same voltages applied as in figure 5a. All SE start on the specimen surface, where it is crossed by the axis of rotation (z-axis, see figure 6a) and have an initial kinetic energy E_{kin}=2eV. The off axis angles are 20° (narrow lines) and 40° (broad lines). Solid lines indicate that the electron travels in the plane of the diagram, the dash-dotted curves are projections of SE-trajectories with azimuthal start angles φ_o of 45°, 90° and 135°.

Figure 7 shows SE-trajectories, if voltages

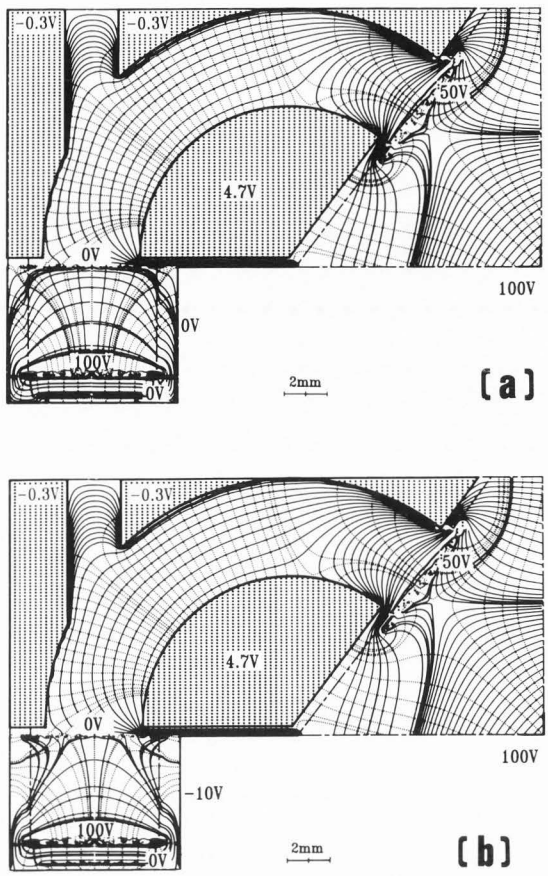

Fig. 5: Equipotential lines (solid lines) and electric field patterns (dotted lines) within the model-spectrometer for different voltages applied to the spectrometer.

are applied to the spectrometer as in figure 5b. The initial energies of the SE are given within the plots. All other initial conditions are the same as in figure 6b. At first, the comparison of figures 6b and 7b shows the already mentioned focusing action on the SE, if a negative voltage is applied to the cylindrical casing. Thereby the SE are forced to pass the retarding grid near the axis so that their transmission through the cylindrical capacitor is enlarged considerably.

Figure 7 also demonstrates the energy selectivity for SE of the spectrometer. Slow SE (fig. 7a) are repelled by the retarding grid or fall upon the inner plate of the cylindrical capacitor, whereas all of the SE with an initial kinetic energy of 2eV (fig. 7b) can pass the spectrometer. The quicker SE of figure 7c cannot be deflected by the weak field of the cylindrical capacitor, and consequently do not contribute to the detectable SE-signal.

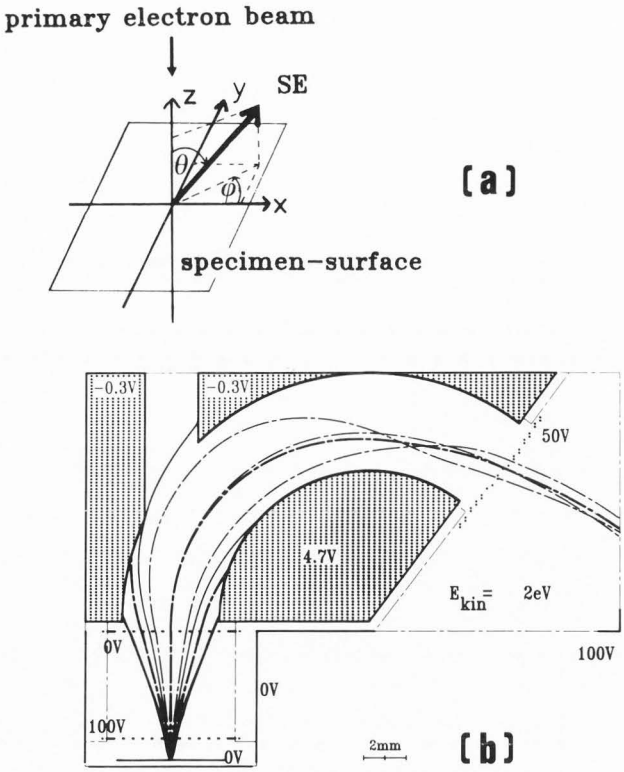

Fig. 6: (a) Coordinate system at the startpoint of the electron trajectories. (b) Simulated electron trajectories within the spectrometer. The same voltages are applied as in figure 5a. For details refer to the main text.

Transmission characteristic of the spectrometer

Transmission ratios were calculated bearing in mind three main considerations:

- They should be the basis for modelling the SE-signal as function of the retarding grid voltage
- The SE-signal curves should be compared for different voltages applied to the specimen
- The influence of the voltage applied to the rotational casing of the retarding part of the spectrometer was to be studied

These considerations led to the simulation of transmission curves for voltages applied to the spectrometer as sketched in figure 8. For U_R values were chosen suitable for building up the SE-signal as a function of U_R using the resulting transmission curves.

Note that the voltages applied to the capacitor part of the spectrometer are coupled with U_R in a way that differences remain constant. This not only considerably reduces the calculation effort but also has the effect that the deflecting property of the capacitor does not depend on the retarding grid voltage.

With this in common two main cases were investigated: in case I the casing of the rotationally symmetrical part is grounded, whereas in case II the casing voltage, too, is coupled to the retarding grid voltage thus providing a constant focusing effect on th SE. In

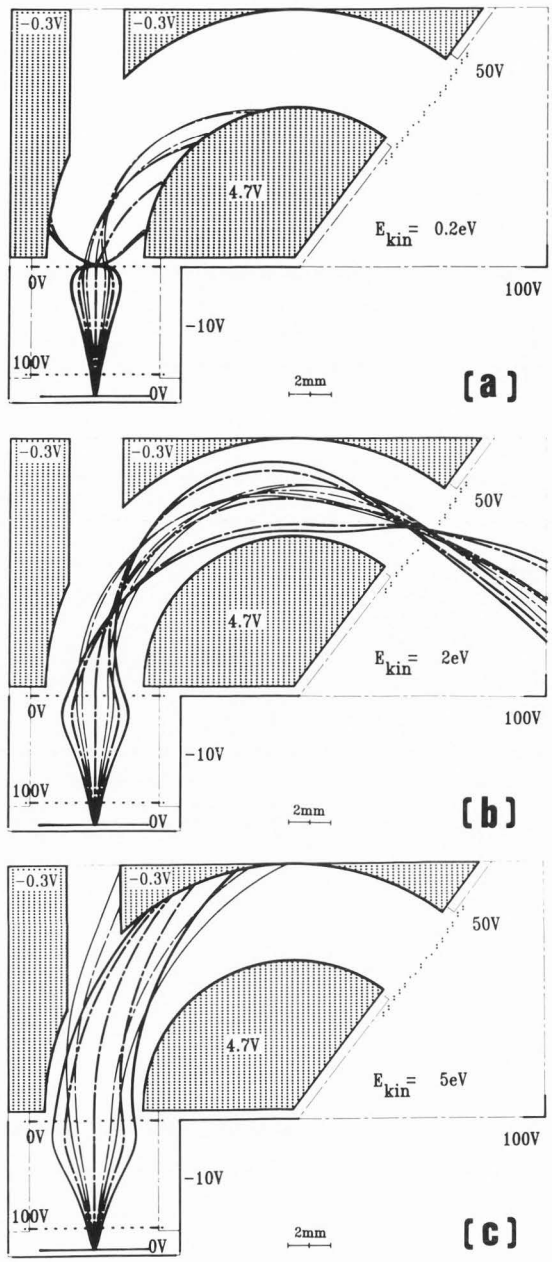

Fig. 7: Simulated electron trajectories within the spectrometer. The same voltages are applied as in figure 5b. For details refer to the main text.

both cases, specimen voltages U_S of 0V and 5V were considered. Figure 9 and figure 10 show calculated transmission curves for these cases.

As expected, all transmission curves show a band-pass characteristic, where the slope on the low-energy side is due to the retarding grid voltage and the slope on the high-energy side is due to the weak deflection field of the 127°-capacitor. For decreasing retarding grid voltages, this transmission maximum is reduced. This reduction can be explained as follows:

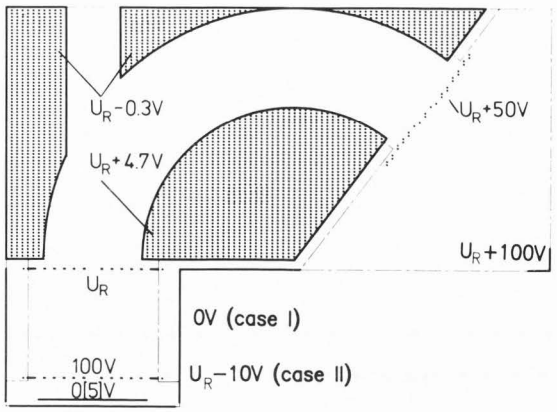

Fig. 8: Voltages applied to the spectrometer for the simulation of its transmission characteristic.

(a) The focusing or defocusing of SE within the retarding part of the spectrometer depends on the voltage difference between retarding grid and casing. Focusing is expected, if the casing is negative, defocusing, if it is positive relative to the retarding grid.
(b) SE of higher energy are not focused to the centre of the retarding grid to the same extent as are the low energy SE.

For case I the decreasing of the transmission maxima with U_R and the different maximum heights of analogous maxima for U_S=0V and U_S=5V is mainly due to (a). In case II the voltage difference between retarding grid and casing is constant. Here the reduction of transmission maxima therefore exclusively is due to (b), and the analogous transmission curves for U_S=0V and U_S=5V are nearly congruent.

The comparison of both cases again confirms that by applying a negative voltage to the cylindrical casing, the SE-transmission of the spectrometer is increased. In addition, it turns out that for the constant voltage difference between casing and retarding grid, the transmission curves no longer depend on the specimen voltage but only on the voltage difference between retarding grid and specimen.

Simulated SE-signal

Using the transmission curves of figure 9 and figure 10, the total SE-transmission $T_{tot}(U_R)$ was evaluated. This is the percentage of the SE-current I_{SE} which is transmitted through the spectrometer and can be detected as the SE-signal. The resulting SE-signal curves are plotted in figure 11. As already could be assumed from the transmission curves, there is an exact linear shift of the signal curves with applied specimen voltage U_S in case II, whereas in case I the shift is only about 4V for a difference in U_S of 5V.

As a linear shift of the measured SE-signal with the specimen voltage is a precondition for quantitative voltage determination, these results show that quantitative voltage measurement techniques using a retarding grid spectrometer can be improved considerably, if the voltage

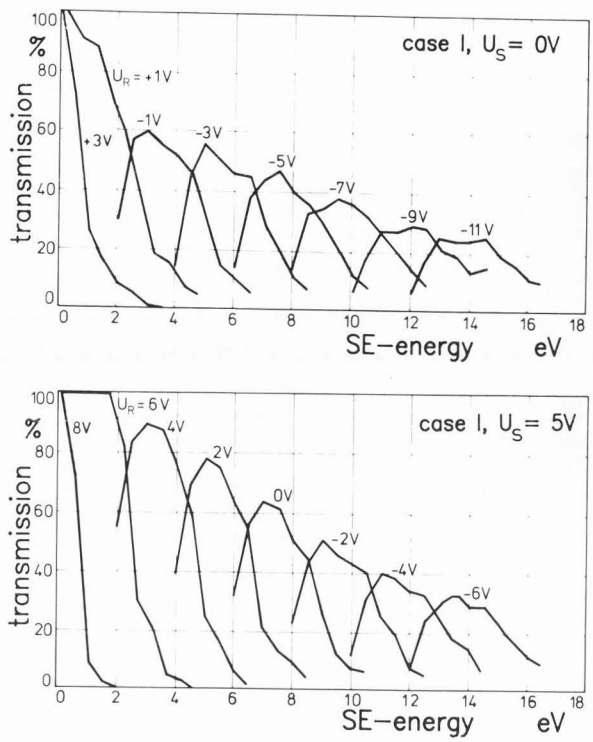

Fig. 9: Transmission characteristic of the 127°-spectrometer for grounded casing (case I).

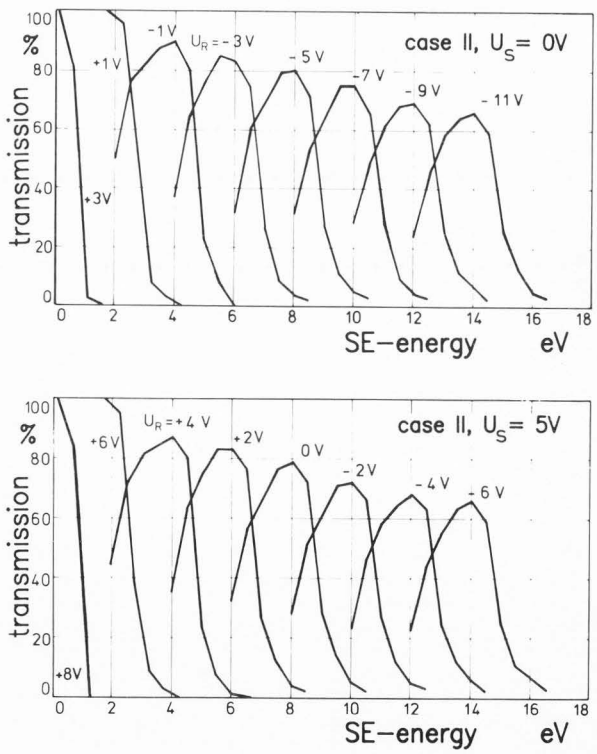

Fig. 10: Transmission characteristic of the 127°-spectrometer for the casing voltage coupled to the retarding grid voltage U_R (case II).

applied to the casing of the retarding part of the spectrometer is at a constant negative level compared with the retarding grid voltage. Due to the focusing action on the SE and the thus improved spectrometer transmission, an enhanced signal to noise ratio for the measurement should be achieved.

Comparison of simulated and experimentally measured SE-signals

For testing the performed computer simulations, the spectrometer depicted in figure 1 was used to experimentally determine the SE-signal as a function of the retarding grid voltage. To match the two-dimensional design employed for the simulations (figure 4), the shielding plates (see figure 1 <e>) were removed and the capacitor exit grid was connected electrically with the capacitor exit plate (see figure 1 <d>). As specimen a Faraday cup was installed. The primary electron energy was 1.1 keV and the primary beam current was 10^{-8}A. A 1 kHz sawtooth voltage was applied to the retarding grid so that the SE-signal as function of the retarding grid voltage could be visualized on an oscilloscope. For that a Tektronix 7854 oscilloscope was used, by means of which the SE-signal could be averaged over several cycles of the ramp voltage applied to the retarding grid (100 cycles for the examples given below). The averaged, digitized signal then was fed into a computer for further processing, such as fitting the signal height to the scale of the simulated data and plotting the results.

Test measurements manifested a strong decrease in signal height with measurement time(in several cases the signal even vanished totally within less than 10sec). As this signal decay is due to negative charging of the ceramic ring (see figure 1 <m>) by backscattered electrons (BE), this ring was replaced by one made of stainless steel, which was electrically connected to the cylindrical casing (see figure 1 <k>).

With this slightly changed spectrometer now the SE-signal-curves were recorded in the manner already described.

The other voltages applied are specified in figure 12 and are close to those values which were used for the simulation of SE-signal-curves (see figure 8).

In figure 13, the measured SE-signal curves for the specimen voltages U_S=0V and U_S=5V are given for two cases. Analogous to the performed simulation of the spectrometer, the difference between the two cases is that the voltage U_{cyl} applied to the cylindrical casing of the lower part of the spectrometer (see figure 1 <k>) is constantly 0V (case I), and that in case II, U_{cyl} is coupled to U_R in a way that $U_{cyl}=U_R-8.8V$. Due to substituting the ceramic ring between extraction- and retarding-grid (see figure 1<m> by one made of stainless steel, no deformation of the measured curves with time occurred. The experimental curves show the expected energy selectivity of the 127°-spectrometer. The shape of the curves and their shifting with the applied specimen voltage (especially, if the peak positions are considered)are in good agreement with the simulated data.

Nevertheless some discrepancies remain. Remarkable is the displacement of the SE-signal peaks to higher retarding grid voltages if compared with the simulated values. The explanation for this should be that even after the elimination of the ceramic ring between extraction- and retarding-grid, the ceramic holders of the retarding - grid had to remain within the spectrometer and were not shielded against BE-bombardment. A negative charge on this holder could be responsible for it that the SE on their way to the 127°-capacitor had to pass a higher potential-barrier than given by the retarding-grid voltage.That is particularly true for SE passing the retarding field far off the axis of the rotationally symmetric part of the spectrometer. This idea is supported by the fact that in case II - where, according to the simulation (see figure 6), these are focused to trajectories near the axis - the discrepancy is considerably lower than in case I.

Other deviations between measured and simulated SE-signals certainly could be avoided, if the simulation is done in three dimensions especially in the region of the grids and the finite-sized 127°-capacitor.

Considering all this, it can be said that the whole simulation process led to a better understanding of the spectrometer properties and to an optimization of the spectrometer design.

Conclusions

A simulation technique has been presented, by which it is possible to predict the performance of SE-spectrometers. By a suitable joining of parts with axial or translational symmetry also sophisticated experimental set-ups can be handled.

As an example, a retarding-field SE-spectrometer was investigated and the simulation data were in acceptable agreement with experimental results. The simulation technique also could be used to achieve a further improvement of the spectrometer.

Nevertheless, it showed up that not all details of a spectrometer simulation can be dealt with by two-dimensional field calculations. As since some time software-programs for three-dimensional field calculations are available, this drawback can be overcome. Then the presented simulation-technique can be used even more advantageously as an aid for the further improvement of SE-spectrometers for e-beam testing, a task which will become the more important the more the size of IC-structures is decreasing.

Acknowledgements

The authors are grateful for financial support of the ministry of science and research of North-Rhine-Westfalia (MWF), of the federal ministry of research and technology (BMFT) and of the Deutsche Forschungsgemeinschaft (DFG).

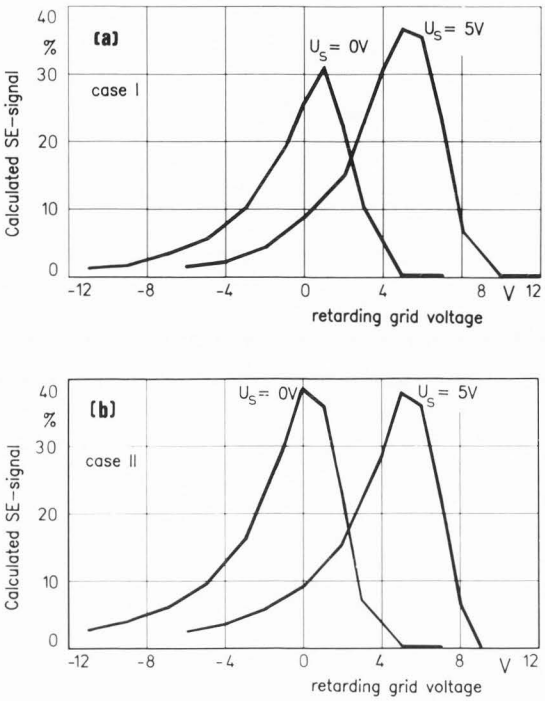

Fig. 11: Calculated SE-signal as function of the retarding grid voltage for earthed casing (case I) and for the casing voltage coupled to the retarding grid voltage U_R (case II).

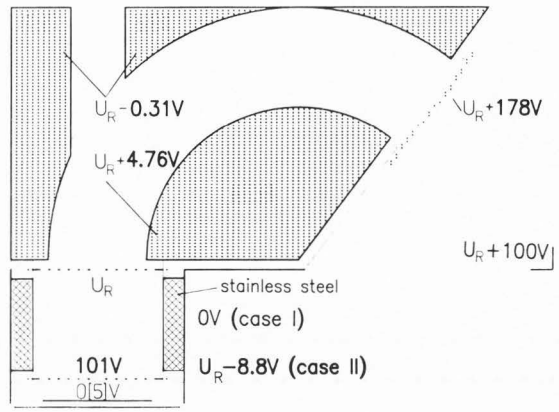

Fig. 12: Voltages applied to the spectrometer for the measurement of SE-signal-curves (see figure 13).

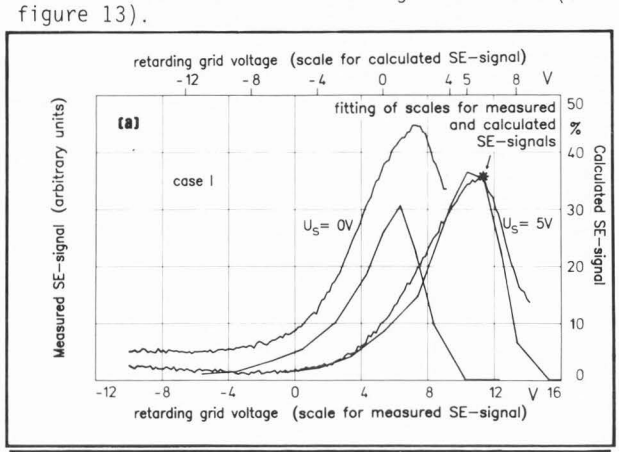

Fig. 13: Measured and simulated SE-signals as function of the retarding grid voltage for constant (case I) and variable (case II) voltage of the cylindrical casing. The voltages applied are as specified in figure 12. The shielding plates (figure 1 <e>) were dismounted. The calculated data are transferred from figure 11, but the abscissae were shifted against each other as depicted. All measured curves were taken under exactly the same experimental conditions, and accordingly processed in the same manner: From all signal-values an equal noise background was subtracted and the scale for the height of the remaining signal was chosen to fit the arrow-marked point of the simulated data.

References

1. Adachi H., Sase M., Zaima S., Shibita Y. (1981). Performance computations for a high-resolution retarding field electron energy analyser with a simple electrode configuration. J. Phys. 14, 769-778.

2. Chung MS., Everhart TE. (1974). Simple calculation of energy distribution of low-energy secondary electrons emitted from metals under electron bombardment. J.Appl.Phys. 45, 707-710.

3. Deutges D., Kubalek E. (1983). Computer aided optimization of electron-spectrometer-detector-design in electron-beam testing systems for integrated circuits. Beitr. elektronenmikroskop. Direktabb. Oberfl. (BEDO) 16,47-56.

4. Dinnis AR., Khursheed A. (1985). Comparison of voltage contrast detectors and surface field effects. Microcircuit Engineering 84. Academic Press London, 433-440.

5. Feuerbaum HP. (1979). VLSI testing using the electron probe. Scanning Electron Microsc. 1979; I: 285-296.

6. Feuerbaum HP. (1983). Electron beam testing: methods and application. Scanning 5, 14-24.

7. Fujioka H., Nakamae K., Ura K. (1981). Local field effects on the voltage measurement using a retarding field analyser in the SEM. Scanning Electron Microsc. 1981; I: 323-332.

8. Gopinath A. (1977). Estimate of minimum measurable voltage in the SEM. J.Phys.E.: Sci.Inst. 10, 911-913.

9. Goto Y., Ito A., Furukawa Y., Inagaki T. (1981). Hemispherical retarding type analyser for IC-testing by electron beam. J.Vac.Sci. Technol., 19, 1030.

10. Khursheed A., Dinnis AR. (1983). Computation of trajectories in voltage contrast detectors. Scanning 5, 25-31.

11. Khursheed A., Dinnis AR. (1984). A comparison of voltage contrast detectors. Scanning 6, 85-95.

12. Kubalek E., Menzel E. (1984). Electron beam microcircuit inspection techniques. From: Methods and materials in microelectronic technology (Plenum Publishing Co.). IBM Research Symposia Series.

13. Menzel E., Kubalek E. (1981). Electron beam test techniques for integrated circuits. Scanning Electron Microsc. 1981; I: 305-322.

14. Menzel E., Brunner M. (1983). Secondary electron analysers for voltage measurements. Scanning Electron Microsc. 1983; I: 65-75.

15. Menzel E., Kubalek E. (1983a). Fundamentals of electron beam testing of integrated circuits. Scanning 5, 103-122.

16. Menzel E., Kubalek E. (1983b). Secondary electron detection systems for quantitative voltage measurements. Scanning 5, 151-171.

17. Munro E. (1973). Computer design of electron lenses by the finite element method. Image Processing and Computer aided design in Electron Optics. London: Academic Press, 284-323.

18. Ostrow M., Menzel E., Postulka E., Görlich S., Kubalek E. (1982). IC-internal electron beam logic state analysis. Scanning Electron Microsc. 1982;II: 563-572.

19. Singer H. (1973). Berechnung von Hochspannungsfeldern mit Hilfe von Flächenladungen. Habilitationsschrift an der TU München. (Calculation of high-voltage fields with the charge density method. Habilitation thesis at the "Technische Universität" in Munich).

20. Steinbigler H. (1969). Anfangsfeldstärken und Ausnutzungsfaktoren rotationssymmetrischer Elektrodenanordnungen in Luft. Dissertation TH München. (Initial field strength and space factor of rotationally symmetric electrode systems in air. Thesis at the "Technische Hochschule" in Munich).

21. Ura K., Fujioka H., Nakamae K., Ishisaka M. (1982). Stroboscopic observation of passivated microprocessor chips by SEM. Scanning Electron Microsc. 1982; III: 1061-1068.

22. Wolfgang E., Lindner R., Fazekas P., Feuerbaum HP. (1979). Electron-beam-testing of VLSI circuits. IEEE J.Solid State Circuits, SC-14, 471-481.

Discussion with Reviewers

E. Munro: Since the potential varies with position on the surface of an operating IC, this will introduce local transverse electric fields near the specimen surface. Do such fields have a significant effect on the performance of the detector, and could they be included in the computer simulation, or would this require a three-dimensional computer program?

H. Fujioka: You mention that local field effects have to be reduced as far as possible. Did you estimate these effects by your program and did you measure them in the experiment?

A.R. Dinnis: Have simulations been made which take account of the transverse fields above real IC specimens?

Authors: In this work no local fields were considered. Nevertheless it is possible to incorporate local fields e.g. above conductor tracks of an IC. Figure 14 shows the two-dimensional electric field above four passivated conductor tracks. The boundary conditions were taken from one mesh of the finite element network of figure 5a just above the specimen surface. Note especially the potential barrier for SE emitted from the +5V conductor track.

A. R. Dinnis: Does the focusing effect of the negative casing voltage improve performance when making measurements on narrow conductors?

Authors: No measurements on narrow conductors were performed.

A. R. Dinnis: Over what area of the specimen are good results achieved?

Authors: This area is given by the center hole of the extraction grid. This grid is a copper mesh with 50µm bars and a center hole of 450µm square.

E. Munro: In the 127° spectrometer, what was the length of the electrodes in the direction normal to the plane of the diagram in figure 5, in units of the inter-electrode spacing? Is it possible to assess the magnitude of the error involved in using a two-dimensional field analysis program that neglects the fringing fields in the transverse direction?

Authors: The length of the electrodes in the normal direction was 12mm, the inter-electrode spacing 5mm. Of course, part of the errors will be due to the two-dimensional simulation. On the

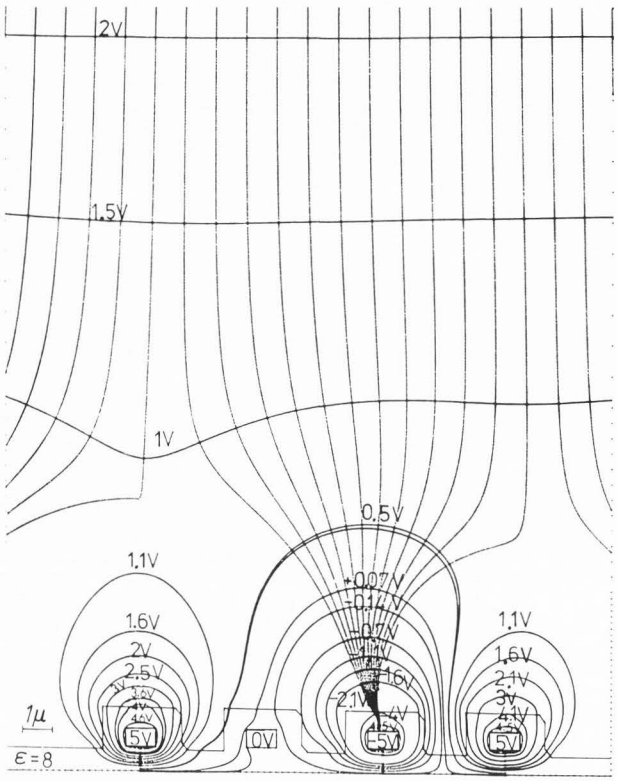

Fig. 14: Local fields at an IC-surface.

other hand, SE-signals curves measured with and without earthed shielding plates (see figure 1 <e>) show no significant differences. The peak position is more or less determined by the voltages applied to the plates of the deflection capacitor (see figure 1 <g> and <h>) as should be expected.

H. Fujioka: What is the total time required to calculate the performance of a spectrometer?

Authors: The total calculation time for a complete SE-signal curve on the used HP 1000 F-computer was about four days. This long calculation time is mainly due to the extensive using of mass-storage for the eliminating of the finite-element matrices. For comparison it may be mentioned that within an analytical rotationally symmetric field a complete SE-signal curve can be obtained in two hours (SE emitted on the axis) resp. 12 hours (SE emitted from an off-axis point).

H. Fujioka: Is it possible to get an optimum design data for a high-performance spectrometer by your program-package?

Authors: In principle yes. Due to the long calculation time needed, it is advisable to start the optimization process with analytical approximations for the design and use the finite element programs only for parts of the design or in the final stage of the optimization process.

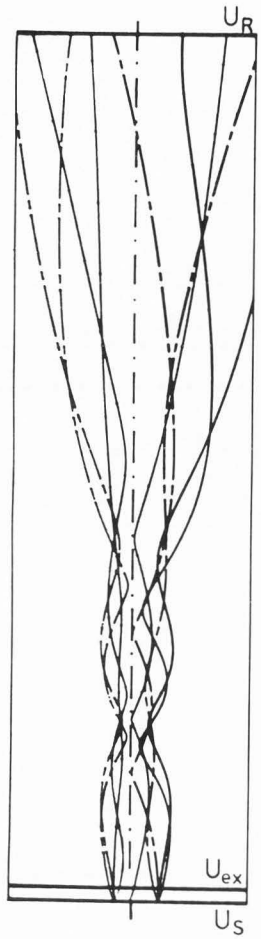

Fig. 15: Electron trajectories in an electromagnetic field.

E. Munro: In figure 5, you show computed electric field lines as well as equipotentials. How are the electric field lines computed in the finite element program?

Authors: Within each of the triangular finite elements the components of the electric field strength are given by the differences of the voltages on the edges of the finite element. Starting from an arbitrary point within the design the direction of the field strength of the finite element there is traced up to the boundary of this element. From here the field direction within the new finite element is taken, and so on. The equipotentials are plotted in a similar way by tracing the directions vertical to the field strength.

A. R. Dinnis: Do you have programs which take account of magnetic as well as electric fields?

Authors: Yes. The programs plotting the electron trajectories and simulating the SE-signal curves are prepared for the consideration of magnetic fields. As an example, figure 15 shows a simple spectrometer set up consisting of a homogeneous extraction field, a homogeneous retarding field and an overlaid magnetic Glaser bell shaped field.

A. R. Dinnis: Could you give a diagram of where the scintillator is situated with respect to the spectrometer? This can have a significant effect on the number of electrons collected, and I have found it worthwhile to simulate trajectories right to the scintillator to ensure accurate predictions.

Authors: In figure 16 the cross-section of the experimental set up with pole piece, spectrometer and the conventional Everhart-Thornley-detector is drawn roughly to scale.

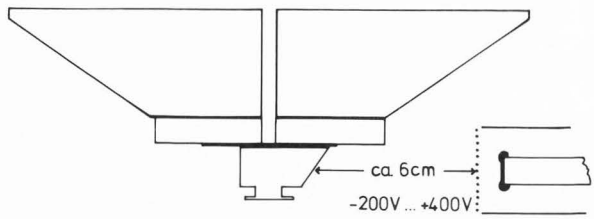

Fig. 16: Experimental set up.